

# Unlocking the Informational Value of Marginal Costs for Exact Time Series Aggregation in Generation Expansion Planning

Luca Santosuosso, Sonja Wogrin  
 Institute of Electricity Economics and Energy Innovation  
 Graz University of Technology  
 Graz, Austria  
 {luca.santosuosso, wogrin}@tugraz.at

**Abstract**—This paper addresses the generation expansion planning (GEP) problem, formulated as a mixed-integer linear programming model with intertemporal storage constraints. Being generally NP-hard, the problem’s computational complexity grows sharply with the planning horizon and the number of binary variables. While previous research has tackled this challenge using heuristic time series aggregation (TSA) methods, we propose a theoretically grounded marginal-cost-based TSA, designed to construct an aggregated model that preserves the active constraints of its full-scale counterpart, thereby explicitly targeting exact temporal aggregation. This TSA method is embedded within solution algorithms that iteratively refine theoretically validated bounds on the maximum error introduced by the temporal aggregation relative to conventional full-scale optimization, thus offering a formal performance guarantee to the decision-maker. Numerical results highlight the computational advantages of the proposed algorithms, which notably recover tractability whereas full-scale optimization proves intractable.

**Index Terms**—Exact time series aggregation, generation expansion planning, energy storage, mixed-integer programming

## I. INTRODUCTION

### A. Literature Review

Generation expansion planning (GEP) is a cornerstone problem in energy system optimization, aiming to determine the optimal mix and sizing of power generation units required to meet future electricity demand while minimizing both capital investment and operational costs [1]. Recently, the large-scale integration of variable renewable energy sources (vRES), the growing deployment of flexible technologies (e.g., energy storage systems), and the evolution of regulatory and market designs have significantly increased the complexity of GEP models [2]. Modern GEP formulations must therefore capture nonlinear system dynamics, alongside intricate intertemporal coupling constraints, over long-term planning horizons [3]. This has driven a steady evolution of GEP models from basic linear programming (LP) formulations [4] toward increasingly complex nonconvex formulations [5], most notably mixed-integer linear programming (MILP) models [6]. Critically, MILP formulations of the GEP problem are strongly NP-hard in general [7], making the trade-off between modeling fidelity and computational tractability a central challenge [8].

To address this trade-off, time series aggregation (TSA) methods are commonly employed [9]. By leveraging clustering techniques, these methods condense the input time series of the GEP problem, such as energy demand profiles or vRES

generation forecasts, into a temporally aggregated counterpart of the original full-scale GEP model, defined over a reduced set of representative time periods (or clusters) [10].

Traditional *a priori* TSA methods rely on standard clustering techniques, such as k-means [11], k-medoids [12], and hierarchical clustering [13], to select representative periods based exclusively on the statistical properties of the input time series. Despite their widespread adoption in GEP [14], the accuracy of these methods is highly case-dependent and must therefore be validated individually for each application [15]. This limitation has motivated growing interest in establishing performance guarantees for aggregated models obtained via TSA [16], typically formulated as bounds on the approximation error relative to the original full-scale model [17]. Although such bounds are valuable for enabling decision-makers to assess the accuracy of an aggregated model [18], they do not allow *a priori* TSA-based models to systematically attain a prescribed level of accuracy. This shortcoming reflects a fundamental limitation of *a priori* methods: they implicitly assume that an accurate statistical representation of the full-scale model’s input space yields a correspondingly accurate approximation of its output solution space. In practice, however, this assumption often fails, as the model outputs depend not only on the input time series but also critically on the underlying mathematical structure of the full-scale model [19].

The recognition of this limitation has led to the recent emergence of the *a posteriori* TSA paradigm [20]. The key distinction of this paradigm from conventional *a priori* TSA is its use of clustering features derived directly from the full-scale model, rather than relying solely on statistical features extracted from the input time series [21]. This paradigm has proven highly effective for GEP [22], particularly in the presence of intertemporal coupling constraints (e.g., due to storage or ramping) [23], which significantly complicate TSA by requiring preservation of temporal chronology to maintain consistency with the full-scale model dynamics [24]. Existing studies have explored *a posteriori* methods based on clustering features derived from approximations of the full-scale primal solution [25] or the dual solution [26]. Nevertheless, a *a posteriori* TSA remains underdeveloped, as the current research has yet to conclusively determine which clustering features most effectively lead to accurate aggregated models.

In this regard, the theoretical result of [27] offers a strong conceptual foundation by demonstrating that, if the decision-maker had prior knowledge of the full-scale model’s active

constraints, TSA could be performed **exactly**, with the aggregated formulation reproducing both the optimal solution space and the optimal objective function value of its full-scale counterpart. Notably, [28] further extends this result to optimization models featuring intertemporal storage constraints.

While perfect knowledge of the full-scale model's active constraint sets during TSA is clearly unattainable, the theoretical result of [27] provides a valuable insight: any clustering feature that reliably captures constraint activation in the full-scale model can be exploited within an a posteriori TSA method to achieve exact temporal aggregation. This highlights a significant, yet largely untapped, opportunity to dramatically reduce the computational complexity of nonconvex GEP models, without compromising solution accuracy.

### B. Research Gaps and Contributions

The literature review reveals the following research gaps:

- Traditional *a priori* TSA methods rely on the frequently violated assumption that an accurate representation of the full-scale model's input space is sufficient to accurately capture its solution space [19]. In contrast, *a posteriori* TSA methods offer greater potential for constructing high-fidelity aggregated models by exploiting information extracted directly from the full-scale model to enrich the clustering feature space [20]. Although prior studies have proposed deriving clustering features from approximations of the full-scale primal [25] and dual [26] solutions, it remains unclear which full-scale model information should be leveraged, and how clustering features should be systematically constructed, to improve the accuracy of temporally aggregated models. This challenge is particularly pronounced for MILP optimization models, where dual information is generally ill-defined.
- Recent analyses [27], [28] demonstrate that exact temporal aggregation can be achieved when the active constraints of the full-scale model are preserved in the aggregated model. These results provide clear theoretical guidance on which aspects of the full-scale model are most critical for ensuring aggregation accuracy and, therefore, should be captured by TSA methods. However, because the set of active constraints is unknown during the TSA process, it remains unclear how this theoretical insight can be translated into practical methods that effectively reduce GEP models while maintaining high solution accuracy and formal performance guarantees.

This paper seeks to address these research gaps through the following **key contributions**:

- We formulate the full-scale GEP model as a MILP problem encompassing multiple generation technologies, including both vRES and thermal power, and subject to intertemporal storage constraints. We then construct the corresponding temporally aggregated model and show that the full-scale model's marginal costs serve as a reliable proxy for identifying the sets of active constraints in the full-scale model, enabling their use as clustering features to achieve exact temporal aggregation.

- Acknowledging that system marginal costs are not directly available during temporal aggregation, we introduce a practical a posteriori TSA method that leverages marginal cost estimates obtained from the dual space of the full-scale model's linear relaxation to guide the construction of the temporally aggregated model.
- We develop two iterative solution algorithms that systematically reduce the temporal dimensionality of the full-scale MILP GEP model while providing a formal performance guarantee in the form of theoretically validated bounds on the approximation error introduced by temporal aggregation. Notably, both algorithms deliver feasible solutions for the full-scale model at each iteration, and the aggregated model is progressively refined toward exact temporal aggregation through the proposed marginal-costs-based a posteriori TSA method.

Finally, the proposed algorithms are evaluated using real-world data from the ENTSO-E Transparency Platform [29].

The remainder of the paper is organized as follows: Section II details the proposed methodology, Section III presents the numerical results, and Section IV concludes the study.

## II. METHODOLOGY

This section presents the proposed methodology. Subsection II-A introduces the full-scale GEP model, while Subsection II-B presents its temporally aggregated counterpart. Subsection II-C details the proposed marginal-cost-based a posteriori TSA method, which is employed in the algorithms of Subsection II-D to iteratively refine bounds on the optimal objective function value of the original full-scale model.

In the following, sets and vectors are denoted in boldface (e.g.,  $\mathbf{z}$ ). The notation  $|\cdot|$  denotes the cardinality of a set.

### A. The Full-Scale Model

The goal is to determine the optimal mix and sizing of generation units that minimize capital investment and operational costs while meeting the energy demand. Specifically, we consider an asset portfolio comprising vRES, namely wind and solar power plants, thermal units, and energy storage systems. In the following formulation, we omit grid constraints, consistent with the operation of generation portfolios that do not participate in the grid management, such as commercial virtual power plants or generation companies [1]. Future work will extend the formulation to incorporate these constraints.

Let  $\mathcal{G}$ ,  $\mathcal{N}$ , and  $\mathcal{T}$  denote the sets of generators (indexed by  $g$ ), energy storage systems (indexed by  $n$ ), and time steps (indexed by  $t$ ), respectively. The operational costs of generator  $g$  and non-supplied energy are denoted by  $C_g^{\text{pg}}$  and  $C^{\text{ns}}$  (€/MWh), respectively. For each storage unit  $n$ ,  $C_n^{\text{pc}}$  and  $C_n^{\text{pd}}$  denote the charging and discharging costs (€/MWh). The investment costs (€/MW) are  $C_g^{\text{g,inv}}$  for generators and  $C_n^{\text{s,inv}}$  for storage units. The input time series comprise the generator capacity factors  $F_{g,t}$  and the energy demand  $D_t$  (MWh).

We denote by  $x_g^{\text{g}}$  and  $x_n^{\text{s}}$  the installed capacities (MW) of generator  $g$  and storage unit  $n$ , respectively. The binary variables  $b_g^{\text{g}}$  and  $b_n^{\text{s}}$  enforce that installed capacities are either zero or lie within  $[\underline{X}_g^{\text{g}}, \overline{X}_g^{\text{g}}]$  and  $[\underline{X}_n^{\text{s}}, \overline{X}_n^{\text{s}}]$ , respectively.

The operational variables include the power output  $p_{g,t}^g$  (MW) of generator  $g$  at time  $t$ , the non-supplied energy  $e_t^{\text{ns}}$  (MWh), the charging and discharging power of storage unit  $n$ , denoted by  $p_{n,t}^c$  and  $p_{n,t}^d$  (MW), respectively, and its stored energy  $e_{n,t}^s$  (MWh) at time  $t$ . The charging and discharging efficiencies of storage unit  $n$  are denoted by  $\eta_n^c$  and  $\eta_n^d$ , respectively,  $T_n$  denotes its energy-to-power ratio (h), while  $E_n^0$  denotes its initial stored energy (MWh).

We group the decision variables of the full-scale model in the set  $\mathbf{z}$ , defined as:

$$\mathbf{z} := \{x_g^g, x_n^s, b_g^g, b_n^s, p_{g,t}^g, e_{n,t}^s, p_{n,t}^c, p_{n,t}^d, e_t^{\text{ns}}\}_{g \in \mathbf{G}, n \in \mathbf{N}, t \in \mathbf{T}}.$$

The objective function of the GEP problem is defined as

$$J(\mathbf{z}) := \sum_{g \in \mathbf{G}} C_g^{\text{g,inv}} x_g^g + \sum_{n \in \mathbf{N}} C_n^{\text{s,inv}} x_n^s + \sum_{t \in \mathbf{T}} \sum_{g \in \mathbf{G}} C_g^{\text{pg}} p_{g,t}^g \Delta + \sum_{t \in \mathbf{T}} \left( \sum_{n \in \mathbf{N}} (C_n^{\text{pc}} p_{n,t}^c + C_n^{\text{pd}} p_{n,t}^d) \Delta + C_n^{\text{ms}} e_t^{\text{ns}} \right), \quad (1)$$

which represents the sum of both capital investment and operational costs over the planning horizon  $\mathbf{T}$ .

The **full-scale GEP model**, formulated as a MILP problem, is defined over  $\mathbf{T}$  with sampling time  $\Delta$  (h) as follows:

$$\min_{\mathbf{z}} J(\mathbf{z}) \quad (2a)$$

$$\text{s.t.} \quad \sum_{g \in \mathbf{G}} p_{g,t}^g \Delta + \sum_{n \in \mathbf{N}} (p_{n,t}^d - p_{n,t}^c) \Delta + e_t^{\text{ns}} = D_t, \quad \forall t, \quad (2b)$$

$$e_{n,t+1}^s = e_{n,t}^s + (\eta_n^c p_{n,t}^c - \eta_n^d p_{n,t}^d) \Delta, \quad \forall n, \forall t \in \mathbf{T} \setminus \{|\mathbf{T}| - 1\}, \quad (2c)$$

$$e_{n,0}^s = E_n^0, \quad \forall n, \quad (2d)$$

$$0 \leq p_{g,t}^g \leq F_{g,t} x_g^g, \quad \forall g, \forall t, \quad (2e)$$

$$0 \leq e_{n,t}^s \leq x_n^s \Delta, \quad \forall n, \forall t, \quad (2f)$$

$$0 \leq p_{n,t}^c \leq \frac{x_n^s \Delta}{T_n}, \quad \forall n, \forall t, \quad (2g)$$

$$0 \leq p_{n,t}^d \leq \frac{x_n^s \Delta}{T_n}, \quad \forall n, \forall t, \quad (2h)$$

$$b_n^s \underline{X}_n^s \leq x_n^s \leq b_n^s \overline{X}_n^s, \quad \forall n, \quad (2i)$$

$$b_g^g \underline{X}_g^g \leq x_g^g \leq b_g^g \overline{X}_g^g, \quad \forall g, \quad (2j)$$

$$e_t^{\text{ns}} \geq 0, \quad \forall t, \quad (2k)$$

$$b_g^g \in \{0, 1\}, \quad \forall g, \quad (2l)$$

$$b_n^s \in \{0, 1\}, \quad \forall n. \quad (2m)$$

In (2), the constraints (2b) enforce the energy balance; (2c) and (2d) characterize the storage dynamics; (2i) and (2j) impose capacity investment limits; and (2e)–(2h) together with (2k)–(2m) define the bounds on the decision variables.

### B. The Temporally Aggregated Model

Mixed-integer GEP problems are known to be strongly NP-hard [7]. As the problem dimension increases with the number of binary variables and time steps, (2) may become computationally intractable. To mitigate this, TSA can be employed to construct an aggregated counterpart of (2), defined over a reduced set of representative periods, denoted by  $\mathbf{K}$  and

indexed by  $k$ . When  $|\mathbf{K}| \ll |\mathbf{T}|$ , the aggregated model offers a significant computational advantage over the full-scale model.

Let  $\mathbf{T}_k$  denote the set of consecutive time steps  $t \in \mathbf{T}$  assigned to the  $k$ -th cluster via TSA. We define  $K := |\mathbf{K}|$  and  $T_k := |\mathbf{T}_k|$ . The aggregated counterparts of  $F_{g,t}$  and  $D_t$  are computed as

$$\hat{F}_{g,k} := \sum_{t \in \mathbf{T}_k} \frac{F_{g,t}}{T_k}, \quad \forall g, \forall k, \quad (3) \quad \hat{D}_k := \sum_{t \in \mathbf{T}_k} \frac{D_t}{T_k}, \quad \forall k. \quad (4)$$

We group the variables of the aggregated model as follows:

$$\hat{\mathbf{z}} := \left\{ \hat{x}_g^g, \hat{x}_n^s, \hat{b}_g^g, \hat{b}_n^s, \hat{p}_{g,k}^g, \hat{e}_{n,k}^s, \hat{p}_{n,k}^c, \hat{p}_{n,k}^d, \hat{e}_k^{\text{ns}} \right\}_{g \in \mathbf{G}, n \in \mathbf{N}, k \in \mathbf{K}}.$$

The aggregated counterpart of  $J(\mathbf{z})$  in (1) is

$$\hat{J}(\hat{\mathbf{z}}) := \sum_{g \in \mathbf{G}} C_g^{\text{g,inv}} \hat{x}_g^g + \sum_{n \in \mathbf{N}} C_n^{\text{s,inv}} \hat{x}_n^s + \sum_{k \in \mathbf{K}} \sum_{g \in \mathbf{G}} C_g^{\text{pg}} \hat{p}_{g,k}^g T_k \Delta + \sum_{k \in \mathbf{K}} \left( \sum_{n \in \mathbf{N}} (C_n^{\text{pc}} \hat{p}_{n,k}^c + C_n^{\text{pd}} \hat{p}_{n,k}^d) \Delta + C_n^{\text{ms}} \hat{e}_k^{\text{ns}} \right) T_k. \quad (5)$$

The **temporally aggregated GEP model**, formulated as a MILP problem, is defined over  $\mathbf{K}$  as follows:

$$\min_{\hat{\mathbf{z}}} \hat{J}(\hat{\mathbf{z}}) \quad (6a)$$

$$\text{s.t.} \quad \sum_{g \in \mathbf{G}} \hat{p}_{g,k}^g \Delta + \sum_{n \in \mathbf{N}} (\hat{p}_{n,k}^d - \hat{p}_{n,k}^c) \Delta + \hat{e}_k^{\text{ns}} = \hat{D}_k, \quad \forall k, \quad (6b)$$

$$\hat{e}_{n,k+1}^s = \hat{e}_{n,k}^s + (\eta_n^c \hat{p}_{n,k}^c - \eta_n^d \hat{p}_{n,k}^d) T_k \Delta, \quad \forall n, \forall k \in \mathbf{K} \setminus \{K - 1\}, \quad (6c)$$

$$\hat{e}_{n,0}^s = E_n^0, \quad \forall n, \quad (6d)$$

$$0 \leq \hat{p}_{g,k}^g \leq \hat{F}_{g,k} \hat{x}_g^g, \quad \forall g, \forall k, \quad (6e)$$

$$0 \leq \hat{e}_{n,k}^s \leq \hat{x}_n^s \Delta, \quad \forall n, \forall k, \quad (6f)$$

$$0 \leq \hat{p}_{n,k}^c \leq \frac{\hat{x}_n^s \Delta}{T_n}, \quad \forall n, \forall k, \quad (6g)$$

$$0 \leq \hat{p}_{n,k}^d \leq \frac{\hat{x}_n^s \Delta}{T_n}, \quad \forall n, \forall k, \quad (6h)$$

$$\hat{b}_n^s \underline{X}_n^s \leq \hat{x}_n^s \leq \hat{b}_n^s \overline{X}_n^s, \quad \forall n, \quad (6i)$$

$$\hat{b}_g^g \underline{X}_g^g \leq \hat{x}_g^g \leq \hat{b}_g^g \overline{X}_g^g, \quad \forall g, \quad (6j)$$

$$\hat{e}_k^{\text{ns}} \geq 0, \quad \forall k, \quad (6k)$$

$$\hat{b}_g^g \in \{0, 1\}, \quad \forall g, \quad (6l)$$

$$\hat{b}_n^s \in \{0, 1\}, \quad \forall n. \quad (6m)$$

In (6), the constraints (6b)–(6m) represent the temporally aggregated counterparts of (2b)–(2m), respectively.

### C. Clustering Based on Marginal Costs

The construction of the aggregated model (6) requires clustering to identify representative periods within the planning horizon  $\mathbf{T}$ . The intertemporal constraints in (2) render standard methods (e.g., k-means) unsuitable, as they neglect temporal chronology; we therefore use a *sliding-window clustering* to group consecutive time steps by clustering feature similarity.

Let  $\{\mathbf{a}_t\}_{t \in \mathbf{T}}$  be the set of clustering features. We evaluate the similarity between consecutive elements of  $\{\mathbf{a}_t\}$ , assigning  $t$  to cluster  $k$  if

$$\|\mathbf{a}_t - \boldsymbol{\mu}_k\|_2 \leq \zeta, \quad (7)$$

---

**Algorithm 1** Marginal Cost–Based Time Series Aggregation with Bounded Objective Function Error
 

---

**Input:** Parameters of (2), optimality threshold  $\epsilon^{\text{thr}}$ , maximum number of iterations  $I := |\mathbf{I}|$ , and similarity threshold  $\zeta$ .  
**Output:** Objective function bounds  $J^{\text{UB}^*}$  and  $J^{\text{LB}^*}$ .

- 1:  $i \leftarrow 1$ ;  $\epsilon^i \leftarrow +\infty$ ;  $J^{\text{LB}^i} \leftarrow -\infty$ ;  $J^{\text{UB}^i} \leftarrow +\infty$ ;
- 1: **while**  $\epsilon^i > \epsilon^{\text{thr}}$  and  $i \leq I$  **do**
- 2: Estimate marginal costs according to Steps I and II of Subsection II-D;
- 3:  $\{\mathbf{T}_k^i\}_{k \in \mathbf{K}^i} \leftarrow$  Sliding-window clustering of Subsection II-C using threshold  $\zeta$  and estimated marginal costs as features;
- 4:  $\hat{\mathbf{z}}^* \leftarrow$  Solve the aggregated model (6) for  $\{\mathbf{T}_k^i\}_{k \in \mathbf{K}^i}$ ;
- 5:  $J^{\text{LB}^{i+1}} \leftarrow \max(\hat{J}(\hat{\mathbf{z}}^*), J^{\text{LB}^i})$ ;
- 6:  $\tilde{J} \leftarrow$  Solve the full-scale model (2) with investment variable values fixed to those in  $\hat{\mathbf{z}}^*$  (LP model);
- 7:  $J^{\text{UB}^{i+1}} \leftarrow \min(\tilde{J}, J^{\text{UB}^i})$ ;
- 8:  $\epsilon^{i+1} \leftarrow 100 \frac{J^{\text{UB}^{i+1}} - J^{\text{LB}^{i+1}}}{J^{\text{UB}^{i+1}}}$ ;
- 9:  $i \leftarrow i + 1$ ;
- 10: **end while**
- 11:  $J^{\text{LB}^*} \leftarrow J^{\text{LB}^i}$  and  $J^{\text{UB}^*} \leftarrow J^{\text{UB}^i}$ ;

---

where  $\boldsymbol{\mu}_k$  denotes the centroid of cluster  $k$ , defined as  $\boldsymbol{\mu}_k := \frac{1}{T_k} \sum_{t \in \mathbf{T}_k} \mathbf{a}_t$ , and  $\zeta$  is a user-defined similarity threshold. If (7) is not met for  $\mathbf{a}_t$ , a new cluster is initialized starting at  $t$ .

The selection of clustering features is a key determinant of the quality of the aggregated model (6). Conventional a priori TSA methods construct these features exclusively from the input time series of the GEP problem. Although this strategy preserves the problem input space, it offers no guarantee that the aggregated model will accurately reproduce the outputs (e.g., the optimal objective function value or the optimal solution space) of the full-scale model [19]. In general, a decision-maker is primarily concerned with preserving accuracy in the GEP model’s output space rather than its input space.

To address this issue, we build on the theoretical results of [27] and [28], which establish that an aggregated model reproduces the exact outputs of its full-scale counterpart when it captures the active constraints of the full-scale model at optimality. In the full-scale model (2), the constraints (2e)–(2h) become active when a generator reaches its operational limits, as dictated by (2i) and (2j), thereby triggering a transition in the marginal generator that sets the system’s marginal cost. Hence, marginal costs provide an effective proxy for constraint activation and can be used as clustering features to guide the construction of (6) toward exact temporal aggregation.

#### D. Practical Solution Algorithms

While Subsection II-C highlighted the potential of marginal cost-based clustering for exact TSA, two fundamental challenges remain. First, the nonconvexity of the full-scale model (2) precludes the computation of marginal costs via duality theory. Second, even if marginal costs were obtainable, their evaluation would require solving the full-scale model itself, thereby negating the computational benefits of TSA.

---

**Algorithm 2** Adaptive Marginal Cost–Based Time Series Aggregation with Bounded Objective Function Error
 

---

**Input:** Parameters of (2), optimality threshold  $\epsilon^{\text{thr}}$ , maximum number of iterations  $I := |\mathbf{I}|$ , and similarity threshold  $\zeta$ .  
**Output:** Objective function bounds  $J^{\text{UB}^*}$  and  $J^{\text{LB}^*}$ .

- 1:  $i \leftarrow 1$ ;  $\epsilon^i \leftarrow +\infty$ ;  $J^{\text{LB}^i} \leftarrow -\infty$ ;  $J^{\text{UB}^i} \leftarrow +\infty$ ;
- 2: **while**  $\epsilon^i > \epsilon^{\text{thr}}$  and  $i \leq I$  **do**
- 3: **if**  $i = 1$  **then**
- 4:  $\hat{\boldsymbol{\lambda}}^i \leftarrow$  Estimate marginal costs according to Steps I and II of Subsection II-D;
- 5: **else**
- 6:  $\hat{\boldsymbol{\lambda}}^i \leftarrow$  Estimate marginal costs based on the discrepancies between  $\tilde{\boldsymbol{\lambda}}^{i-1}$  and  $\hat{\boldsymbol{\lambda}}^{i-1}$ , as detailed in Subsection II-D;
- 7: **end if**
- 8:  $\{\mathbf{T}_k^i\}_{k \in \mathbf{K}^i} \leftarrow$  Sliding-window clustering of Subsection II-C using threshold  $\zeta$  and  $\hat{\boldsymbol{\lambda}}^i$  as features;
- 9:  $\hat{\mathbf{z}}^* \leftarrow$  Solve the aggregated model (6) for  $\{\mathbf{T}_k^i\}_{k \in \mathbf{K}^i}$ ;
- 10:  $J^{\text{LB}^{i+1}} \leftarrow \max(\hat{J}(\hat{\mathbf{z}}^*), J^{\text{LB}^i})$ ;
- 11:  $\{\tilde{\boldsymbol{\lambda}}^i, \tilde{J}\} \leftarrow$  Solve the full-scale model (2) with investment variable values fixed to those in  $\hat{\mathbf{z}}^*$  (LP model);
- 12:  $J^{\text{UB}^{i+1}} \leftarrow \min(\tilde{J}, J^{\text{UB}^i})$ ;
- 13:  $\epsilon^{i+1} \leftarrow 100 \frac{J^{\text{UB}^{i+1}} - J^{\text{LB}^{i+1}}}{J^{\text{UB}^{i+1}}}$ ;
- 14:  $i \leftarrow i + 1$ ;
- 15: **end while**
- 16:  $J^{\text{LB}^*} \leftarrow J^{\text{LB}^i}$  and  $J^{\text{UB}^*} \leftarrow J^{\text{UB}^i}$ ;

---

To overcome these, we propose the following marginal cost estimation procedure, executed over  $i \in \mathbf{I}$  iterations.

**Step I.** For each month in the GEP horizon, randomly sample  $i$  days. Next, solve a surrogate linear model obtained by relaxing the binary variables in (2) to continuous variables in the interval  $[0, 1]$ . This surrogate model is defined at full-scale temporal resolution but only over the set of sampled days. For instance, if  $i = 2$  and the full-scale model is formulated at hourly resolution, the surrogate model spans 576 time steps (i.e., 2 sampled days per month over 12 months, with 24 hours per day). This optimization step yields an estimate of the marginal cost trajectory for each sampled day.

**Step II.** For each month, all non-sampled days are assigned, with equal probability, to one of the  $i$  sampled days of that month. Each non-sampled day is assumed to share the same marginal cost trajectory as the sampled day to which it is assigned. For example, if a particular day is assigned to a sampled day  $d$ , the hourly marginal costs of  $d$  are used as a proxy for the marginal costs of that day. This step yields a marginal cost estimate over the full-scale horizon  $\mathbf{T}$ , which is then used as a feature in the sliding-window clustering of Subsection II-C to construct the aggregated model (6).

Importantly, irrespective of the clustering technique employed, the aggregated model (6) provides, by construction, a lower bound on the optimal objective function value of the full-scale model (2) [30]. Fixing the investment variables in (2) to those computed via (6) reduces (2) to a linear

program, whose solution yields an upper bound on the full-scale optimal objective. At each iteration  $i \in \mathbf{I}$ , the relative difference between the upper and lower bounds, denoted  $J^{UB^i}$  and  $J^{LB^i}$ , respectively, defines the optimality gap  $\epsilon^i$ , indicating that the MILP GEP solution derived via TSA is at most  $\epsilon^i$  suboptimal. Convergence is achieved when  $\epsilon^i$  falls below a prescribed threshold  $\epsilon^{thr}$ . This iterative procedure, which combines marginal cost-based a posteriori TSA with bound-based error evaluation, constitutes the proposed Algorithm 1.

Algorithm 1 refines the aggregated model by progressively increasing the number of sampled days used to estimate marginal costs. However, the optimization steps employed to compute the objective function bounds also generate additional, underexploited information. Specifically, solving (2) with fixed investment variables to obtain an upper bound on the objective function produces short-run marginal cost estimates, which can be used to enhance the TSA as follows.

Let  $\tilde{\lambda}^i$  denote the marginal costs obtained from the optimization step yielding  $J^{UB^i}$  (i.e., the short-run marginal costs), and let  $\hat{\lambda}^i$  denote those used to construct the aggregated model at iteration  $i$  (i.e., the long-run marginal costs). Algorithm 2 introduces an adaptive alternative to Algorithm 1 executing the above Steps I and II at iteration  $i + 1$  over the days exhibiting the largest average hourly deviation between  $\tilde{\lambda}^i$  and  $\hat{\lambda}^i$ , rather than over randomly sampled days as in Algorithm 1, adapting TSA to the observed optimality gap.

Critically, both Algorithms 1 and 2 exhibit the following key properties. First, they are accompanied by a formal performance guarantee, in the form of theoretically validated bounds on the objective function error incurred relative to the original full-scale GEP model (2). Second, at each iteration, they yield a feasible solution for (2), i.e., the decision variable values employed to compute the objective function upper bound. Finally, they offer two complementary and practical strategies to exploit the theoretical results of [27] and [28], thereby guiding the construction of the aggregated model toward exact temporal aggregation based on marginal cost estimates.

### III. NUMERICAL RESULTS

This section presents the numerical results. Subsection III-A describes the case study, Subsection III-B illustrates how marginal-cost-based clustering enables exact TSA, and Subsection III-C compares the proposed solution algorithms.

#### A. Case Study Description

To ensure transparency and reproducibility, we generate the problem parameters from prescribed distributions as follows.

For each storage unit, the charging and discharging efficiencies are set to 0.9 and 1/0.9, respectively, while the associated operational costs are drawn from a uniform distribution over  $[5, 15]$  €/MWh. Capacity investment costs are sampled uniformly from  $[4.5 \times 10^5, 5.5 \times 10^5]$  €/MW, and storage capacity investments are either zero or constrained to  $[0.25, 1]$  MW. The stored energy is initialized to 0 MWh, with the energy-to-power ratio fixed at 2 h. Among the generators, 20% are thermal units, 40% wind, and 40% solar. Capacity investments in thermal and vRES units are either zero or constrained to

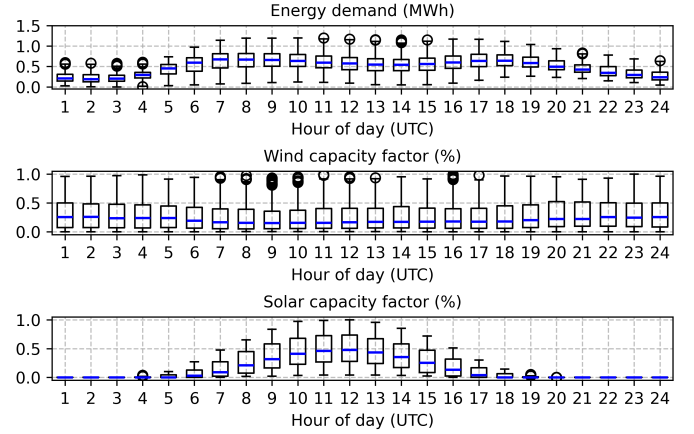


Fig. 1. Boxplots of the hourly input data. Each boxplot characterizes the distribution of values observed at a given hour: the box spans the interquartile range, the blue line indicates the median, the whiskers extend to the 10th and 90th percentiles, and the outliers are shown as individual points.

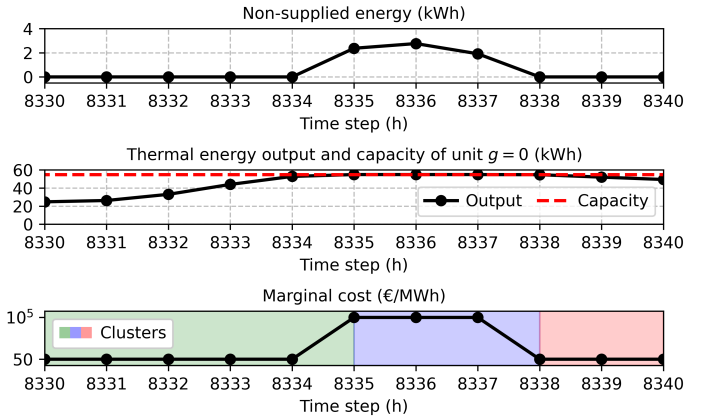


Fig. 2. Example of marginal-cost-based time series aggregation.

$[0.5, 1]$  MW and  $[0.2, 1]$  MW, respectively. The investment costs are sampled uniformly from  $[3 \times 10^6, 4 \times 10^6]$  €/MW for thermal units and  $[5 \times 10^5, 6 \times 10^5]$  €/MW for vRES. The operational costs are set to 50 €/MWh for thermal units and 1 €/MWh for vRES, while the cost of non-supplied energy is  $10^5$  €/MWh. The GEP horizon is one year with hourly resolution ( $|\mathbf{T}| = 8760$ ). In the proposed algorithms, we set  $I = 25$ ,  $\zeta = 10$  and  $\epsilon^{thr} = 0.01\%$ .

The capacity factor of thermal units is fixed at 1, whereas vRES capacity factors and the energy demand time series are derived by scaling real-world observations from the Austrian power grid in 2024, available on the ENTSO-E Transparency Platform [29], and illustrated in Fig. 1. The baseline demand profile shown in Fig. 1 is scaled by a factor  $0.05 (|\mathbf{G}| + |\mathbf{N}|)$  in order to reflect the aggregate system size. To generate heterogeneous production profiles across vRES units, uniform multiplicative noise in the range  $[0.85, 1.15]$  is applied to the baseline wind and solar capacity factors depicted in Fig. 1.

The optimization models are implemented on an Intel i7 processor with 32 GB of RAM, using Gurobi 12.0.1.

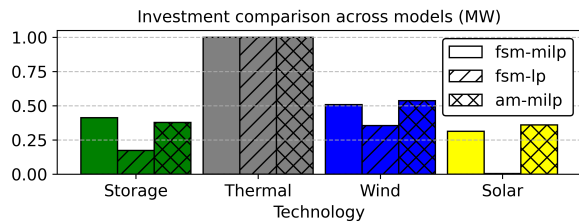


Fig. 3. Comparison of investment decisions obtained with the full-scale MILP model (fsm-milp), its LP relaxation (fsm-lp), and the proposed aggregated MILP model (am-milp).

### B. Using Marginal Costs for Exact Time Series Aggregation

Fig. 2 illustrates how marginal costs can be used to identify active constraints in the LP relaxation of the full-scale GEP model (2), with  $|\mathcal{G}| = 5$  and  $|\mathcal{N}| = 0$ . When the marginal generator (the only available thermal unit) reaches its maximum capacity (at  $t = 8335$ ), the marginal cost increases from  $50 \text{ €}$  (its operating cost) to  $10^5 \text{ €}$ , corresponding to the non-supplied energy penalty. Conversely, as demand decreases and the generator operates strictly within its feasible region (starting from  $t = 8338$ ), the marginal cost decreases from  $10^5 \text{ €}$  back to  $50 \text{ €}$ . Hence, marginal costs alone constitute a sufficient statistic to identify the active constraint sets of the GEP problem, specifically whether the upper limit on thermal power generation or the lower limit on non-supplied energy is binding. This example illustrates that using marginal costs as clustering features for TSA yields an aggregated model that preserves the full-scale active constraints, thereby resulting in exact temporal aggregation, as demonstrated in [27].

When addressing the MILP GEP model (2), marginal costs obtained from its LP relaxation are used as proxies for the true marginal costs within the proposed solution algorithms (see Subsection II-D). Clearly, the LP relaxation could, in principle, serve directly as an approximation of the original MILP GEP model rather than solely for estimating marginal costs. However, Fig. 3 shows that, for an illustrative stylized system comprising both storage ( $|\mathcal{N}| = 1$ ) and generation ( $|\mathcal{G}| = 10$ ) units, the combination of TSA based on marginal cost estimates from the LP relaxation with the construction of an aggregated model that preserves the nonconvex investment constraints, as proposed, provides a substantially more accurate approximation of the MILP GEP model’s optimal investment decisions than the conventional LP relaxation.

### C. Comparative Performance of the Proposed Algorithms

To illustrate the performance of the proposed solution algorithms, Fig. 4 reports the convergence of their objective function bounds for a GEP model with  $|\mathcal{G}| = 100$  and  $|\mathcal{N}| = 10$ . As detailed in Subsection II-D, both algorithms execute the same TSA and optimization steps during the first iteration. From the second iteration onward, a key distinction emerges: Algorithm 2 leverages the upper-bound information obtained in the previous iteration to refine marginal cost estimates, whereas Algorithm 1 does not. This difference is evident in Fig. 4, where Algorithm 2 achieves a  $\sim 3\%$  optimality gap by the second iteration, while Algorithm 1 exhibits a  $\sim 10\%$  gap.

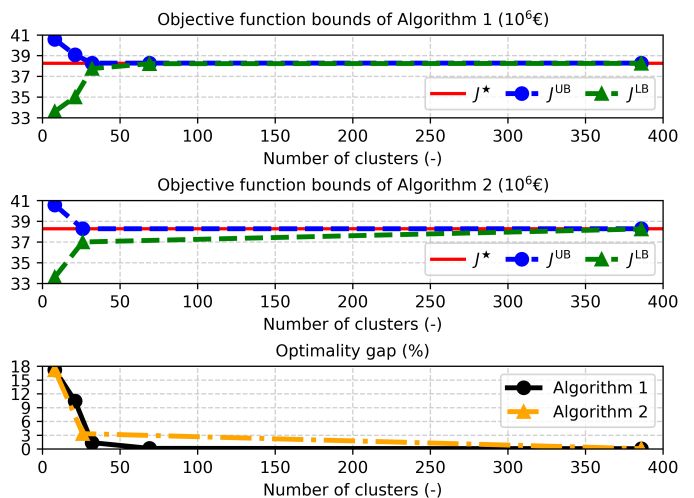


Fig. 4. Performance comparison of the proposed Algorithms 1 and 2.

TABLE I  
COMPARISON BETWEEN THE RUNTIMES OF THE FULL-SCALE MODEL, ALGORITHM 1, AND ALGORITHM 2 AS  $|\mathcal{N}|$  AND  $|\mathcal{G}|$  INCREASE. RELATIVE DIFFERENCES WITH RESPECT TO THE FULL-SCALE MODEL ARE REPORTED IN BRACKETS. THE SYMBOL  $\infty$  INDICATES INTRACTABLE INSTANCES OF THE FULL-SCALE MODEL.

$ \mathcal{N} $	$ \mathcal{G} $	Runtime (min)		
		Full-scale model	Algorithm 1	Algorithm 2
50	50	2.1	2.9 (+38%)	2.4 (+14%)
250	250	51.9	22.4 (−57%)	19.6 (−62%)
750	750	432.8	211.1 (−51%)	102.3 (−76%)
1500	1500	$\infty$	291.9 (− $\infty$ )	144.2 (− $\infty$ )

Notably, both algorithms ultimately converge to over 99.99% accuracy using 386 clusters, corresponding to a reduction of more than 95% in the temporal dimension of the GEP model. However, Algorithm 1 requires five iterations to reach convergence, whereas the adaptive Algorithm 2 converges in only three iterations, achieving the same dimensionality reduction with lower computational effort.

Finally, Table I reports the computational performance of the proposed algorithms in comparison with conventional full-scale optimization. As anticipated, Algorithm 2 consistently exhibits faster runtimes than Algorithm 1. While for small instances of the GEP problem the TSA-based algorithms may incur higher computational costs relative to full-scale optimization, their efficiency increases markedly as the number of generation and storage units, and consequently the number of binary variables, grows. Notably, both algorithms maintain tractability, whereas conventional full-scale optimization proves intractable, i.e., it fails to solve within the prescribed time of 24 hours.

## IV. CONCLUSION AND FUTURE WORK

This paper addresses the GEP problem, formulated as a MILP model incorporating intertemporal storage constraints. Being NP-hard, the problem’s computational complexity increases sharply with the planning horizon and the number of generators. To address this challenge, we propose a novel a posteriori TSA method that leverages marginal cost estimates

to ensure the aggregated model retains the active constraints of the full-scale model, thereby targeting exact temporal aggregation. The TSA method is embedded within solution algorithms that iteratively refine theoretically validated bounds on the maximum error introduced by the temporal aggregation, while producing a feasible GEP solution at each iteration.

Numerical results show the potential of marginal-cost-based clustering for exact TSA and the efficiency of the proposed algorithms, which restore tractability where the full-scale model proves intractable. Future work will aim to refine the marginal cost estimation procedure while incorporating additional nonconvex dynamics in the GEP problem.

## V. AI USAGE DISCLOSURE

AI was utilized for spelling and grammar checking.

### REFERENCES

- [1] A. Baringo, L. Baringo, and J. M. Arroyo, "Robust virtual power plant investment planning," *Sustain. Energy Grids Netw.*, vol. 35, pp. 101105, Sept. 2023.
- [2] N. E. Koltsaklis and A. S. Dagoumas, "State-of-the-art generation expansion planning: A review," *Appl. Energy*, vol. 230, pp. 563–589, Nov. 2018.
- [3] V. N. Motta, M. F. Anjos, and M. Gendreau, "Survey of optimization models for power system operation and expansion planning with demand response," *Eur. J. Oper. Res.*, vol. 312, no. 2, pp. 401–412, Jan. 2024.
- [4] B. F. Hobbs, "Optimization methods for electric utility resource planning," *Eur. J. Oper. Res.*, vol. 83, no. 1, pp. 1–20, May 1995.
- [5] J. F. Franco, M. J. Rider, and R. Romero, "A mixed-integer quadratically-constrained programming model for the distribution system expansion planning," *Int. J. Electr. Power Energy Syst.*, vol. 62, pp. 265–272, Nov. 2014.
- [6] C. L. Lara, D. S. Mallapragada, D. J. Papageorgiou, A. Venkatesh, and I. E. Grossmann, "Deterministic electric power infrastructure planning: Mixed-integer programming model and nested decomposition algorithm," *Eur. J. Oper. Res.*, vol. 271, no. 3, pp. 1037–1054, Dec. 2018.
- [7] S. Goderbauer, M. Comis, and F. J.L. Willamowski, "The synthesis problem of decentralized energy systems is strongly NP-hard," *Comput. Chem. Eng.*, vol. 124, pp. 343–349, May 2019.
- [8] C. Li, A. J. Conejo, P. Liu, B. P. Omell, J. D. Siirola, and I. E. Grossmann, "Mixed-integer linear programming models and algorithms for generation and transmission expansion planning of power systems," *Eur. J. Oper. Res.*, vol. 297, no. 3, pp. 1071–1082, Mar. 2022.
- [9] S. Pineda and J. M. Morales, "Chronological time-period clustering for optimal capacity expansion planning with storage," *IEEE Trans. Power Syst.*, vol. 33, no. 6, pp. 7162–7170, Nov. 2018.
- [10] R. Granell, C. J. Axon, and D. C. H. Wallom, "Impacts of raw data temporal resolution using selected clustering methods on residential electricity load profiles," *IEEE Trans. Power Syst.*, vol. 30, no. 6, pp. 3217–3224, Nov. 2015.
- [11] N. Sarajpoor, L. Rakai, J. Arteaga, N. Amjady, and H. Zareipour, "Time aggregation in presence of multiple variable energy resources," *IEEE Trans. Power Syst.*, vol. 39, no. 1, pp. 587–601, Jan. 2024.
- [12] T. Schütz, M. H. Schraven, M. Fuchs, P. Remmen, and D. Müller, "Comparison of clustering algorithms for the selection of typical demand days for energy system synthesis," *Renew. Energy*, vol. 129, pp. 570–582, Dec. 2018.
- [13] Y. Liu, R. Sioshansi, and A. J. Conejo, "Hierarchical clustering to find representative operating periods for capacity-expansion modeling," *IEEE Trans. Power Syst.*, vol. 33, no. 3, pp. 3029–3039, May 2018.
- [14] F. D. Munoz, B. F. Hobbs, and J.-P. Watson, "New bounding and decomposition approaches for MILP investment problems: Multi-area transmission and generation planning under policy constraints," *Eur. J. Oper. Res.*, vol. 248, no. 3, pp. 888–898, Feb. 2016.
- [15] L. Kotzur, P. Markewitz, M. Robinius, and D. Stolten, "Impact of different time series aggregation methods on optimal energy system design," *Renew. Energy*, vol. 117, pp. 474–487, Mar. 2018.
- [16] L. Santosuosso and S. Wogrin, "Optimal virtual power plant investment planning via time series aggregation with bounded error," in *2025 IEEE PES Innovative Smart Grid Technologies Conference Europe (ISGT Europe)*, Valletta, Malta, 2025, pp. 1–5.
- [17] D. F. Rogers, R. D. Plante, R. T. Wong, and J. R. Evans, "Aggregation and disaggregation techniques and methodology in optimization," *Oper. Res.*, vol. 39, no. 4, pp. 553–582, Aug. 1991.
- [18] W. W. Tso, C. D. Demirhan, C. F. Heuberger, J. B. Powell, and E. N. Pistikopoulos, "A hierarchical clustering decomposition algorithm for optimizing renewable power systems with storage," *Appl. Energy*, vol. 270, pp. 115190, July 2020.
- [19] M. Sun, F. Teng, X. Zhang, G. Strbac, and D. Pudjianto, "Data-driven representative day selection for investment decisions: A cost-oriented approach," *IEEE Trans. Power Syst.*, vol. 34, no. 4, pp. 2925–2936, July 2019.
- [20] M. Hoffmann, L. Kotzur, D. Stolten, and M. Robinius, "A review on time series aggregation methods for energy system models," *Energies*, vol. 13, no. 3, pp. 641, Feb. 2020.
- [21] C. Li, A. J. Conejo, J. D. Siirola, and I. E. Grossmann, "On representative day selection for capacity expansion planning of power systems under extreme operating conditions," *Int. J. Electr. Power Energy Syst.*, vol. 137, pp. 107697, May 2022.
- [22] K. Poncelet, H. Höschle, E. Delarue, A. Virag, and W. D'haeseleer, "Selecting representative days for capturing the implications of integrating intermittent renewables in generation expansion planning problems," *IEEE Trans. Power Syst.*, vol. 32, no. 3, pp. 1936–1948, May 2017.
- [23] D. A. Tejada-Arango, M. Domeshek, S. Wogrin, and E. Centeno, "Enhanced representative days and system states modeling for energy storage investment analysis," *IEEE Trans. Power Syst.*, vol. 33, no. 6, pp. 6534–6544, Nov. 2018.
- [24] L. Kotzur, P. Markewitz, M. Robinius, and D. Stolten, "Time series aggregation for energy system design: Modeling seasonal storage," *Appl. Energy*, vol. 213, pp. 123–135, Mar. 2018.
- [25] Y. Zhang, V. Cheng, D. S. Mallapragada, J. Song, and G. He, "A model-adaptive clustering-based time aggregation method for low-carbon energy system optimization," *IEEE Trans. Sustain. Energy*, vol. 14, no. 1, pp. 55–64, Jan. 2023.
- [26] D. Cardona-Vasquez, T. Klatzer, B. Klinz, and S. Wogrin, "Enhancing time series aggregation for power system optimization models: Incorporating network and ramping constraints," *Elect. Power Syst. Res.*, vol. 230, pp. 110267, May 2024.
- [27] S. Wogrin, "Time series aggregation for optimization: One-size-fits-all?," *IEEE Trans. Smart Grid*, vol. 14, no. 3, pp. 2489–2492, May 2023.
- [28] T. Klatzer, D. Cardona-Vasquez, L. Santosuosso, and S. Wogrin, "Towards exact temporal aggregation of time-coupled energy storage models via active constraint set identification and machine learning," *arXiv preprint*, 2025. [Online]. Available: <https://arxiv.org/abs/2510.14451>.
- [29] L. Hirth, J. Mühlpenfordt, and M. Bulkeley, "The ENTSO-E Transparency Platform—A review of Europe's most ambitious electricity data platform," *Appl. Energy*, vol. 225, pp. 1054–1067, Sept. 2018.
- [30] L. Santosuosso, B. Klinz, and S. Wogrin, "What are we clustering for? Establishing performance guarantees for time series aggregation in generation expansion planning," *arXiv preprint*, 2025. [Online]. Available: <https://arxiv.org/abs/2510.09357>.